Roman-era alluvial waste in the Vistre de la Fontaine (Nîmes, southeast France): from a sacred spring to a contaminated river

Clément Flaux, Sabrina Save, Maxime Scrinzi, Nicolas Minvielle Larousse, Christophe Vaschalde, Audrey Renaud, Margaux Tillier, Abel Guihou, Pierre Deschamps, Alain Véron

Journal of Roman Archaeology 36 (2023), 1–24
doi:10.1017/S1047759423000132

Roman-era alluvial waste in the Vistre de la Fontaine (Nîmes, southeast France): from a sacred spring to a contaminated river

Clément Flaux[1], Sabrina Save[2], Maxime Scrinzi[1], Nicolas Minvielle Larousse[3], Christophe Vaschalde[1], Audrey Renaud[1], Margaux Tillier[4], Abel Guihou[5], Pierre Deschamps[5], and Alain Véron[5]

[1]Mosaïques Archéologie, Cournonterral (France) <c.flaux@mosaiquesarcheologie.com> <m.scrinzi@mosaiquesarcheologie.com> <c.vaschalde@mosaiquesarcheologie.com> <a.renaud@mosaiquesarcheologie.com>
[2]Amélie France, Troyes (France) <save@ameliefrance.com>
[3]École Française de Rome, Rome (Italy); Aix Marseille Univ, CNRS, LA3M, Aix-en-Provence (France) <minvielle.nicolas@gmail.com>
[4]Ipso Facto scop, Marseilles (France) <margaux.tillier@ipsofacto.coop>
[5]Aix Marseille University, CNRS, IRD, INRAE, CEREGE, Aix-en-Provence, France <guihou@cerege.fr> <deschamps@cerege.fr> veron@cerege.fr

Abstract: The excavation of a palaeochannel at the Vistre de la Fontaine 2-2 archaeological site, 3 km downstream from the ancient city of Nîmes (southeastern France), provided an accumulation sequence covering the last 2,500 years. Trace metal analyses of these alluvial sediments disclosed lead (Pb) contamination during the Early Roman Empire, with concentrations close to 1,000 ppm, a factor of 100 above the local geochemical background. This excess of Pb shows a uniform isotopic signature that may reflect unchanged ore sources, either from the Massif Central or from Great Britain. The Pb peak accompanied visible waste that was transported in the sediments of the Vistre de la Fontaine at the time of the development of the Nîmes urban water supply and drainage network during the Early Roman Empire. This research shows the bimillennial persistence of palaeo-contamination in a peri-urban alluvial plain and the relevance of fluvial sedimentary archives in documenting ancient waste.

Keywords: Geoarchaeology, lead, isotopes, palaeopollution, waste, Early Roman Empire

There have been many discoveries of Roman lead (Pb) palaeo-contamination in urban sedimentary archives throughout the Mediterranean basin.[1] Indeed, Pb resistance to corrosion, its malleability, and the low melting temperature made it the raw material of choice during antiquity for, inter alia, piping, architecture, glassware, crockery, and paint.[2] The use of *plumbum* was so prevalent during Roman antiquity that Pb-Ag ore mining was the main source of Pb contamination detected in Greenland ice cores.[3] The Roman atmospheric Pb peak has therefore been considered a possible chronostratigraphic marker.[4] Moreover, Pb has four stable isotopes of masses 204, 206, 207, and 208, the last three of which are the end products of the Uranium (^{238}U and ^{235}U) and Thorium (^{232}Th) radioactive decay chain. The relative quantity of ^{238}U, ^{235}U, and ^{232}Th in Pb ores varies according

[1] Le Roux et al. 2003; Nin et Leguilloux, 2003; Leroux et al. 2005; Véron et al. 2006; Stanley et al. 2007; Elmaleh et al. 2012; Delile et al. 2014, 2015, 2016, 2017, 2019; Stock et al. 2016; Fagel et al. 2017; Véron et al. 2018; Salel et al. 2019.

[2] Nriagu 1983.

[3] Hong et al. 1994; McConnel et al. 2018.

[4] Renberg et al. 2001.

Fig. 1 - Colour online, B/W in print

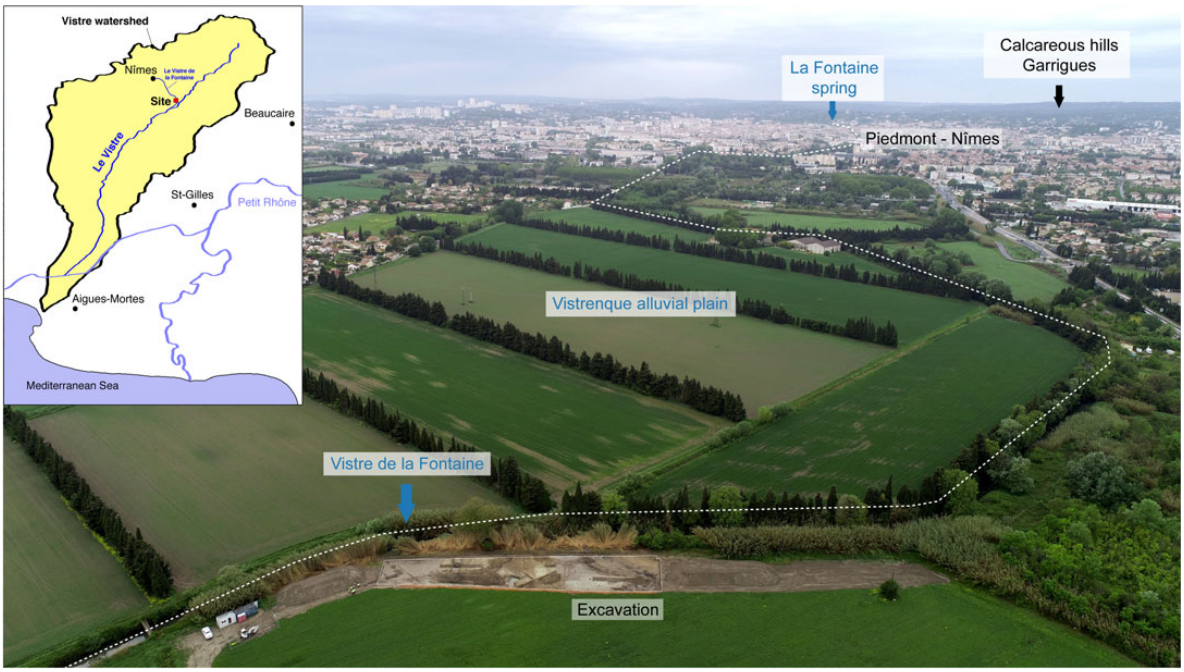

Fig. 1. *Aerial view looking northwards from the Vistre de la Fontaine 2-2 site under excavation, in the Vistrenque plain, at the foot of the Nîmes limestone hills, northwest of the Rhône delta. The insert top-left shows the geographical context of the Vistre de la Fontaine, a tributary of karstic origin of the Vistre coastal river, itself a tributary of the Rhône-Sète canal. (Photo © Globdrone.)*

to the age of the source rock and its initial U and Th concentrations.[5] As such, isotopic imprints coupled with concentration analyses provide a marker of anthropogenic activities, as well as of the geographical origin of the ores used in the manufacture of urban artifacts, when compared to the Pb isotopic signature database of known deposits. In that respect, anthropogenic lead in sediments constitutes a proxy for the expansion and contraction of ancient urban development.[6] Here we used this geochemical indicator in sediments of the Vistre de la Fontaine palaeochannel to document the environmental footprint of Nemausus (Nîmes, southeastern France) during antiquity.

Archaeological assessment carried out as part of a project to restore the meandering trajectory of the Vistre de la Fontaine stream on the outskirts of rural Nîmes led to the excavation of a palaeochannel in the watercourse and of a bridge dating back to the Early Roman Empire (Fig. 1). The excavation area opened a 2,500-year time window on the evolution of a section of the palaeo-Vistre de la Fontaine. Archaeology, stratigraphy, sedimentology, and malacology of this alluvial sequence together show the migration of the minor bed and its convex bank over an approximate length of 30 m.[7] The accretion of this bank therefore featured a sequence of sedimentary archives that was investigated following a multiproxy approach. Granulometry, sedimentology, and analyses of major and trace elements and Pb isotopic signatures made it possible to test for the presence and origin of metallic palaeo-pollutants recorded in the alluvial sediments during the historical period, in connection with the development of the city located approximately 3 km upstream from

5 Doe 1970.

6 Delile, 2014; Delile et al. 2016, 2017.

7 Flaux et al. 2022.

the site. Additional data include anthracological, archaeozoological, and carpological remains found within the Roman-period minor bed of the river. Originating from a sacred karstic spring that became a central node in the development of the Nîmes agglomeration from the end of the 6th c. BCE, the Vistre de la Fontaine River displays today physico-chemical indications of domestic and agricultural contaminants (sewage waters and high nitrate levels, respectively).[8] This study explores for the first time the deep history of anthropogenic contamination of this urban river.

Methods

Chronostratigraphy

The Vistre de la Fontaine is a karstic river flowing from a perennial spring which constituted the heart of Nîmes from its foundation in the 6th c. BCE. The Vistre de la Fontaine 2-2 site, located ca. 3 km downstream from the city, allowed the excavation of a Roman bridge that used to cross the river and opened a window onto the evolution of its palaeochannel over the last 2,500 years. A stratigraphic section of about 40 m in length with a deep dig and three auger cores intersected the accreting palaeo-bank over a length of about 30 m (see stratigraphic transect in Fig. 2), producing a temporal sedimentary series that was horizontally structured. This section underwent a detailed stratigraphic field survey and an orthorectified and georeferenced photogrammetric survey. Thirty-three samples of raw sediment were taken horizontally along the convex bank's lateral accretion. The granulometry of the deposits was approximated using wet sieving and fraction quantification of gravel (> 2mm), coarse sand (> 0.5 mm), fine sand (> 0.063 mm), and silt and clay (< 0.063 mm) (Table 1). The composition of sand and gravel fractions were observed using binocular loupes. The chronology of this sequence was established on the basis of stratigraphic relationships, archaeological structures in situ, and archaeological artifacts in secondary positions, as well as by three radiocarbon dates (Table 2).

Bio-archaeology

Fluvial deposits that filled the Roman palaeochannel as a result of stable hydromorphic conditions provided a sequence of carpological, anthracological, and zoological data from the Roman period. The samples were prepared and studied at Mosaïques Archéologie laboratory. Details of the bioarchaeological methods and studies employed on the Vistre de la Fontaine 2-2 site can be found in the excavation report.[9]

Nine samples of approximately 10 L were selected for anthracology, from which 360 charcoals were extracted after wet sieving of bulk sediments through mesh of 4, 1, and 0.5 mm. Four samples of approximately 10 L were selected for carpology, from which ca. 8,000 remains were extracted after wet sieving of bulk sediments through mesh of 4, 1, and 0.35 mm. One thousand and forty-nine archaeozoological fragments were collected during the excavation and after wet sieving of bulk sediment sampled from the fluvial context (both minor bed and bank) of the Roman era.

---

8 Maréchal et al. 2004.

9 Scrinzi et al. 2021.

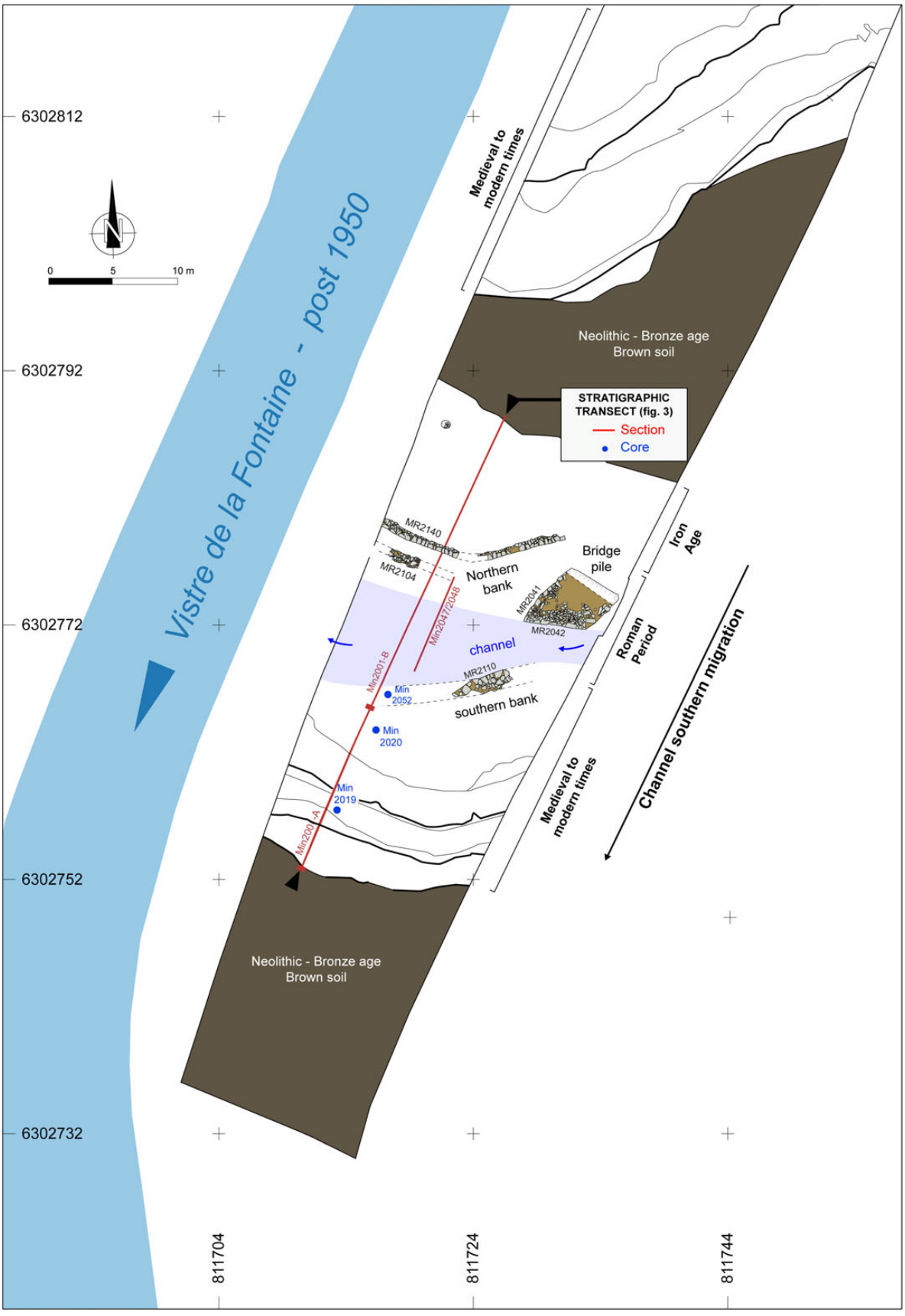

Fig. 2 - Colour online, B/W in print

Fig. 2. *General Holocene phasing of the stripped surface, map of the Early Roman Empire remains, and location of the stratigraphic sections. Lambert 93 coordinate system. (Map by C. Flaux.)*

Table 1.
Granulometric data and XRF data applied along the accretionary profile of the convex bank of the Vistre de la Fontaine palaeochannel (samples 1–33; Fig. 3). Measurements were made on two certified sediment standards (NIST Standard 2710a and NIST Standard 2711a) at the beginning and end of the analysis, enabling the error bar to be calculated for each element (**).

Sample			*Granulometry*						*XRF concentration (ppm) (** % of error on certified standards)*										
			Dry sample mass (g)						*Ca*	*Fe*	*K*	*Ti*	*Sr*	*Pb*	*Zr*	*Cu*	*Zn*	*Rb*	*Th*
Distance (m)	*Id LAB*	*Stratigraphic unit*	*Total*	*> 2 cm*	*> 2 mm*	*> 0.5 mm*	*> 0.063 mm*	*< 0.063 mm*	*** 38.8*	*** 12*	*** 8.7*	*** 7.1*	*** 22.6*	***0.95*	*** 7*	*** 7.9*	*** 4.6*	*** 2.5*	*** 10.4*
38.36	**1**	2002	155.1	0.0	0.0	2.9	21.7	130.5	236598	8205	7560	1006	699	9.5	95.4	11	23.8	29.8	13
37.55	**2**	2093	142.2	0.0	49.0	28.7	20.1	44.4	247704	5832	6560	863	366	18.5	68.2	13	20.4	23.1	9.3
37	**3**	2093	147.2	0.0	0.0	9.7	31.4	106.1	225247	5762	7417	1174	378	17.1	95.5	14	20.6	28.2	13.8
36.38	**4**	2093	144.7	0.0	0.0	4.4	63.5	76.8	168726	8892	9502	1428	245	17.3	115.9	15	29.6	36.6	9.4
35	**5**	2024	154.3	0.0	41.2	42.5	36.7	33.9	282007	4561	6027	783	261	9	79.5	12	15.7	16	9.9
34	**6**	2095	118.0	0.0	0.0	8.7	57.5	51.8	167158	6901	7638	1581	247	14.7	128.5	9	21.9	31.4	9
33	**7**	2095	148.3	0.0	0.0	4.9	48.3	95.1	183000	7195	8681	1593	246	17.2	133.1	16	24.3	33.2	10.9
32	**8**	2095	175.4	0.0	0.0	6.0	71.1	98.3	187718	9417	7490	1494	262	12.1	137	9	18.6	26.1	10.3
31	**9**	2095	159.6	0.0	2.5	25.1	62.9	69.1	210408	7353	7864	1180	261	22.7	85.9	14	21.2	25.9	9.7
30	**10**	2096	156.8	0.0	0.0	1.3	38.4	117.1	152815	8590	8886	1602	228	21.8	136.6	12	27.4	36.5	10.1
29	**11**	2096	153.0	0.0	0.0	3.6	49.8	99.6	154195	9193	8347	1344	257	25.7	129.5	17	34.1	37.5	11
28	**12**	2096	154.8	0.0	0.0	3.6	41.0	110.2	133281	11106	9673	1621	247	27.3	145	26	41.6	42.6	9.1
27	**13**	2097	151.5	0.0	0.0	3.7	46.4	101.4	127452	10089	9416	1720	242	81.4	143.6	29	38.1	40.9	10.6
26	**14**	2097	133.3	0.0	0.0	4.0	36.1	93.2	123487	11689	10552	1934	247	72.7	164	35	39.9	46.8	11.6
25	**15**	2097	219.4	0.0	0.0	3.2	66.6	149.6	114603	13670	10001	1680	268	678	159	277	103	49.7	11.7
24	**16**	2097	151.8	0.0	0.0	1.9	34.9	115.0	118811	13180	10500	1710	270	761	145	196	82	50.7	11.3
23	**17**	2097	159.3	0.0	0.0	3.4	40.3	115.6	119209	13831	10533	1636	276	943	125.5	154	86	50.7	13.8
22	**18**	2098	163.8	0.0	1.0	6.2	65.5	91.1	124020	11900	10168	1635	266	788	144	75	58.6	46.8	15.1
21	**19**	2098	159.1	0.0	0.0	10.6	57.3	91.2	136166	11823	10384	1914	270	784	136.1	80	58.9	40.4	10.7
20	**20**	2098	159.8	0.0	8.1	8.3	53.5	89.9	151543	10286	9019	1656	270	292	140	40	34.8	35.9	11.4
19	**21**	2098	183.7	0.0	1.2	3.0	50.8	128.7	144002	9992	9036	1469	270	157	154	22	36.9	40.6	11.6
18	**22**	2098	149.3	0.0	2.8	8.5	44.7	93.3	176969	8702	8427	1317	297	129	134.8	21	30.2	33.5	13.3
17	**23**	2098	323.1	0.0	2.2	9.8	117.0	194.1	160008	10622	7855	1441	305	130	152	21	27.2	31.6	13.2
16	**24**	2099	325.0	0.0	2.1	15.3	122.1	185.5	164417	9123	8027	1383	309	191	124.4	22	28.3	33.5	14.8
15	**25**	2099	163.4	0.0	0.0	2.9	50.2	110.3	176040	8630	8393	1396	287	170	127.6	21	28.5	33.4	11.7

(*Continued*)

Table 1. Continued.

Sample			*Granulometry*						*XRF concentration (ppm) (** % of error on certified standards)*										
Distance (m)	*Id LAB*	*Strati-graphic unit*	*Dry sample mass (g)*						*Ca*	*Fe*	*K*	*Ti*	*Sr*	*Pb*	*Zr*	*Cu*	*Zn*	*Rb*	*Th*
			Total	*> 2 cm*	*> 2 mm*	*> 0.5 mm*	*> 0.063 mm*	*< 0.063 mm*	*** 38.8*	*** 12*	*** 8.7*	*** 7.1*	*** 22.6*	*** 0.95*	*** 7*	*** 7.9*	*** 4.6*	*** 2.5*	*** 10.4*
14	**26**	2099	197.4	0.0	1.2	2.4	44.6	149.2	189469	7391	8304	1373	283	148	122	25	31.6	33.2	10.5
13	**27**	2099	208.7	0.0	0.0	4.0	61.8	142.9	195446	6849	7804	1157	288	148	108.6	13	25.6	31.1	11.1
12	**28**	2099	150.4	0.0	0.0	4.1	37.5	108.8	197573	6500	7931	1168	297	146	98.4	25	27.5	30.9	11.4
11	**29**	2076	328.5	0.0	1.6	14.9	82.4	229.6	207529	6101	7645	1276	315	119	106.1	20	25.1	27.5	12.3
10	**30**	2076	255.3	0.0	1.4	9	52.7	192.2	181419	6671	8530	1287	298	102.1	127.2	29	28.2	35	12.6
9	**31**	2050	249.1	0.0	1.2	4.0	59.0	184.9	188996	7599	8148	1237	322	86.2	110.2	19	27.7	33.8	12.7
8	**32**	2050	287.4	0.0	0.0	0.0	82.4	205.0	186711	8434	8747	1326	325	89.5	113.4	21	27.8	33	13.8
7	**33**	2050	183.0	0.0	4.0	21.0	57.9	100.1	188948	9243	8815	1279	340	92.3	104.8	25	36.3	36.1	14.1

Table 2.
Samples selected for radiocarbon dating (Calibration carried out according to Reimer et al. 2020).

Minute	*Stratigra-phic unit*	*Sample number*	*Distance (m)*	*CIRAM laboratory code*	*Nature*	*Species*	*Presence of the last tree ring*	*Radiocarbon age BP*		*corrected pMC*		*δ13C (□)*	*Calibrated year BCE / CE*	
2001	2096	2011	25.6	AR14	Charcoal twigs	*Fagus sylvatica, Arbutus unedo, Quercus coccifera/ilex*	yes	2003	± 26	72.92	± 0.26	−24.39	−49	+79
	2097	2013	22	AR15	Wheat caryopsis	*Triticum aestivum/ turgidum*	–	1906	± 25	78.87	± 0.25	−23.45	+64	+213
	2098	2014	17	AR16	Charcoal	*Fagus sylvatica*	no	1901	± 25	78.92	± 0.25	−25.82	+69	+214

Geochemistry

XRF geochemical analysis was performed upon the 33 samples taken along the convex bank's lateral accretion. The raw sediment samples were dried in a heating cabinet at 35°C for ten days, then ground in an agate mortar and compacted into a dish covered by a 4µm-thick polypropylene film used specifically for XRF analysis. Measurements were taken using an InnovX Delta Premium spectrometer equipped with a silicon drift detector (SDD) and a 4W X-ray tube with a rhodium target operating between 10 and 40 kV for a maximum amperage of 200µA. Soil mode was selected with a long exposure time for better accuracy.[10] The raw data from the analysis are presented in Table 1.

Stable lead isotope ratios were measured using a Neptune+ MC-ICPMS (Multi-Collector Inductively Coupled Plasma Mass Spectrometer) at CEREGE (CNRS, France), after microwave-associated digestion of sediments and Pb extraction and purification on AG1X8 resins.[11] The isotope ratios provided in Table 3 were normalized by multiple analyses of the NBS981 standard.[12] Analytical uncertainties (standard deviation) for the measured Pb isotope ratios presented in figures and tables was lower than 0.012%.

Sedimentary archives

General stratigraphy of the Vistrenque

The archaeological site is located on the lower Vistre de la Fontaine River, a tributary of the Vistre coastal river. The alluvial plain of the Vistrenque forms a depression 5 to 7 km wide, extending in a northeast–southwest direction and separating the Garrigues area in the north from the Costières de Nîmes in the south (Fig. 1). The hills and plateaus of the Garrigues region are formed of marly limestone from the Lower Cretaceous, and their piedmont plain is commensurate with a detrital glacis formed during the Pleistocene and Holocene.[13] The Costières to the south comprise series of alluvial terraces formed by the Rhône during the Lower and Middle Pleistocene. These terraces also form the bedrock of the Vistrenque, which would have subsided through synsedimentary tectonic processes.[14]

The main lines of the surface formations of the Vistre plain are now well understood, thanks to the numerous geoarchaeological and palaeoenvironmental studies carried out in this area.[15] The ante-Holocene substratum of the sedimentary sequence consists of the detrital formation of the Costières, the roof of which lies around 3.5 m below the surface, covered by a "loessic complex," deposited over a thickness of 2 to 2.5 m and dated to the recent Pleistocene, with a roof that is capped by a palaeosoil formed during the Tardiglacial period. The Holocene is represented by a pedosedimentary sequence of fine alluvial deposits 0.8 to 1.25 m thick, characterized by a shelly brown palaeosoil, which, in the Vistrenque, is generally defined by occupations from the Neolithic and the Bronze Age.

---

10 Kilbride et al. 2006.

11 Manhès et al. 1978.

12 Doucelance and Manhès 2001. The entire procedure for lead isotopic analysis is detailed in Gelly et al. 2019.

13 Fabre and Monteil 2011.

14 Ménillet and Paloc 1973.

15 Chevillot et al. 2008; Chevillot et al. 2010; Jallet et al. 2017.

Table 3.
Lead isotope ratios. Preparation and analysis of samples took place at CEREGE (CNRS, UMR7730), on a Neptune+ MC-ICPMS (Multi-Collector Inductively Coupled Plasma Mass Spectrometry). The reproducibility of these measurements is associated with an error bar lower than 0.012% for all reported lead isotope ratios.

Sample number	*Distance (m)*	*208Pb/ 204Pb*	*208Pb/ 206Pb*	*208Pb/ 207Pb*	*206Pb/ 207Pb*	*207Pb/ 204Pb*	*206Pb/ 204Pb*
2	37.55	38.659	2.07900	2.46745	1.18685	15.667	18.595
5	35	39.269	2.06947	2.50025	1.20816	15.706	18.975
7	33	38.844	2.06424	2.47685	1.19988	15.683	18.818
8	32	38.906	2.06236	2.47913	1.20209	15.693	18.865
11	29	38.729	2.07373	2.47155	1.19184	15.670	18.676
13	27	38.657	2.08493	2.46624	1.18289	15.674	18.541
15	25	38.632	2.09055	2.46551	1.17936	15.669	18.479
17	23	38.553	2.09097	2.46129	1.17710	15.664	18.438
19	21	38.576	2.09114	2.46209	1.17739	15.668	18.448
20	20	38.554	2.08899	2.46236	1.17873	15.657	18.456
21	19	38.619	2.08890	2.46396	1.17955	15.674	18.488
23	17	38.601	2.08885	2.46396	1.17958	15.666	18.479
25	15	38.553	2.08834	2.46241	1.17913	15.657	18.461
28	12	38.599	2.08951	2.46312	1.17880	15.671	18.473
30	10	38.634	2.08849	2.46403	1.17981	15.679	18.498
31	9	38.571	2.08751	2.46320	1.17997	15.659	18.477
17	23	38.542	2.08871	2.46221	1.17882	15.653	18.453

The construction of the meander

The palaeochannel of the Vistre de la Fontaine was created in a silty alluvial plain. The stripped surface of the site, cleared to about 50 cm below the present soil, reveals this dichotomy in the form of a winding pathway nested in the shelly brown palaeosoil (Fig. 2). Stratigraphic transect 1 (Fig. 3) intersects this formation in a north-northeast–south-southwest direction, showing the truncation of the Neolithic brown, shelly palaeosoil[16] and the underlying loess complex in the form of a 39 m-long basin with a maximum depth of 2 m below the stripped surface. Overall, the basin contains two main sedimentary facies. At the bottom, deposits are mostly coarse, lenticular conglomerates of rolled and joined gravels interspersed with more sandy or even muddy lenticular bodies, which are consistent with the filling of an active minor bed. The upper part is much more homogeneous, composed of massive and monotonous yellowish-brown to greyish-brown sandy silts over a length of more than 30m, intersected by oxidized rhizoconcretions. The homogeneity of this facies is also evident in its texture. Granulometry is mainly fine, with 53 to 77% of silt and clay, 24 to 36% fine sands (Table 1). The sand fraction is invariably composed of abundant, poorly rolled carbonate rhizoconcretions (interpreted as detrital travertines), calcareous and quartz minerals, and malacofaunal elements (shells, shell fragments, and operculum in variable proportions). However, the apparent homogeneity of this layer is structured in multi-metric sedimentary units with oblique interfaces with a 15 to 20° southward inclination, marked by strandlines composed of charcoals or shells left by a high-water level (Fig. 3). This geometry evokes the slope of a fluvial channel bank, and the horizontal succession of deposits provides evidence for the southward accretion of

[16] Chevillot et al. 2010.

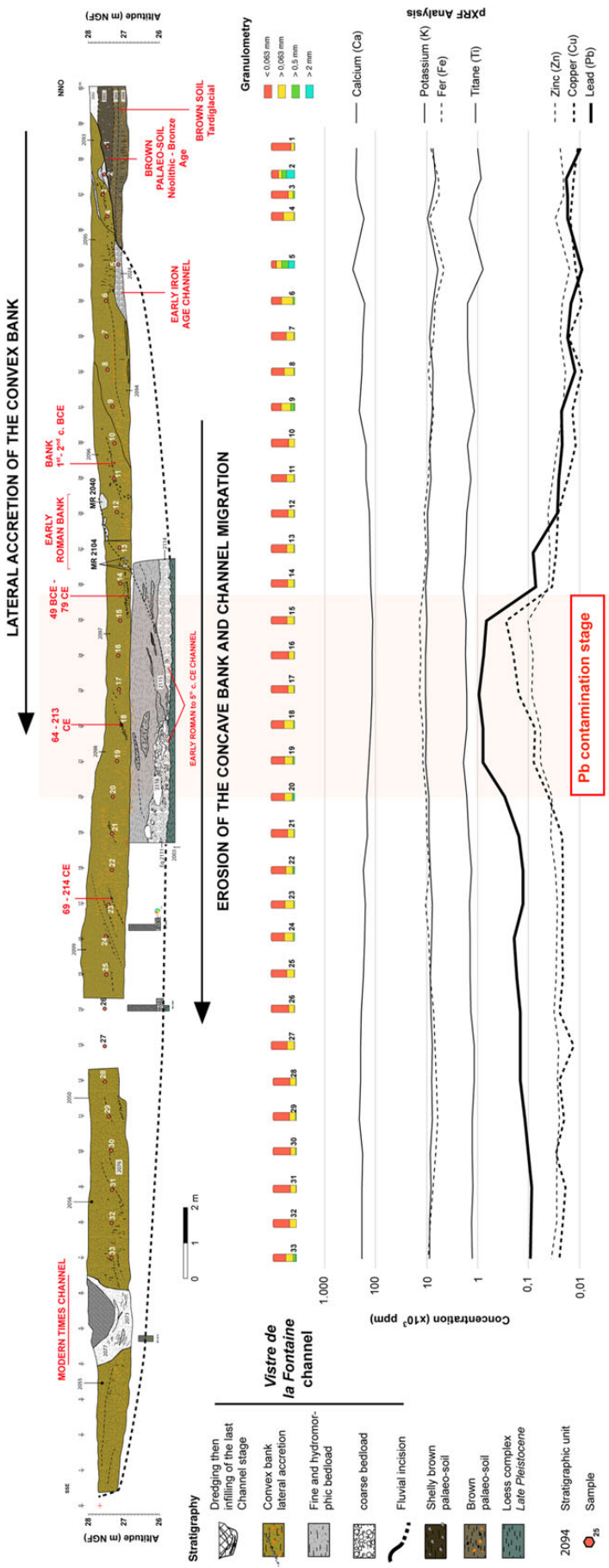

Fig. 3. *South-southeast–north-northwest stratigraphic transect intersecting the palaeochannel of the Vistre de la Fontaine and the southward migration of its convex bank. Location of discrete samples and chronological, granulometric, and geochemical data (XRF) are also shown. (C. Flaux.)*

Fig. 3 - Colour online, B/W in print

this bank, burying the deposits of the Vistre de la Fontaine palaeochannel, jointly migrating towards the south through the erosion of the concave bank. This mechanism reflects the construction of a meander. The malacofauna studied along this sequence shows mixed assemblages composed of aquatic and terrestrial fauna in variable proportions, consistent with the transitional space constituted by these alluvial palaeobanks.[17] The geoarchaeological study of the site, via analysis of anthracological, carpological, palynological, malacological, and archaeozoological alluvial assemblages, has revealed that the Vistrenque formed a diversified mosaic landscape, an open and cultivated alluvial plain where wooded areas nevertheless remained.[18]

Chronology of the meander

The stratigraphy of this homogeneous sedimentary series, structured in multi-metric units with oblique interfaces and a southward inclination of 15 to 20°, and marked by strandlines composed of charcoals or shells left by a high-water level, implies the chronological succession of the deposits of this bank in a southward accretion, burying the laterally and jointly migrating channel deposits. It was possible to date three phases of deposition for these successive channels (Fig. 3). The first, on the north side, is coarsely lenticular and yielded a series of non-rolled ceramic fragments in a good state of preservation, favoring the hypothesis of a rubbish tip in the palaeochannel of the Vistre de la Fontaine. The assemblage yielded hand-thrown pottery, fragments of Etruscan amphorae, and Eastern Greek ceramics dated to the 6th c. BCE.[19] The second phase of channel deposits corresponds to the fluvial activity contemporary with the construction of the bridge and dated to the Early Roman Empire (1st–2nd c. CE).[20] The ceramic assemblage associated with the deposit of this ancient palaeochannel reveals a wider time period, between the 2nd c. BCE and the 5th c. CE, although the overwhelming majority of the ceramics are dated to the Early Roman Empire. Finally, the third phase corresponds to the final sealing of the palaeochannel, traces of which are still visible on contemporary aerial images. The final phase of the filling is anthropic, incorporating fragments of contemporary ceramics and iron elements (nails, rods, barbed wire), providing a terminus post quem of the first half of the 20th c., consistent with the mechanical rectification of the channel carried out between 1945 and 1953.[21]

The accretion of the convex bank of the Vistre de la Fontaine palaeochannel thus took place between the First Iron Age and the contemporary period. One of the oblique interfaces marking the slope of this palaeobank is highlighted in sections by walls MR2040 and, about 1 m below and 2 m farther south, MR2104 (Fig. 3). This construction of the bank of the ancient palaeochannel is associated with the addition of the bridge during the Early Roman Empire, consistent with a ceramic assemblage dated to the 2nd–1st c. BCE and discovered within the bank sediments underlying these two walls.[22] Finally, three radiocarbon dates were ascertained from organic material (Table 2) taken from

17 Scrinzi et al. 2021; Flaux et al. 2022.
18 Scrinzi et al. 2021.
19 Scrinzi et al. 2021.
20 Scrinzi et al. 2021.
21 Scrinzi et al. 2021.
22 Scrinzi et al. 2021.

oblique strandlines composed of charcoals left by a high-water level made after these two walls. From north to south, these three charcoal-bed dates are 49 BCE–79 CE, 64–213 CE, and 69–214 CE, respectively. These bank deposits bury the minor-bed deposits of the ancient palaeochannel, dated by the ceramic assemblages to between the 2nd c. BCE and the 5th c. CE, and are therefore stratigraphically subsequent. The radiocarbon dates appear to contradict the chronological model based on the ceramic material. However, it must be considered that in a fluvial environment, sedimentary stocks can be reformed when transiting along the longitudinal profile of the river. For example, during the accretion of the convex bank of the Vistre de la Fontaine, the sedimentary material is likely a result of an eroding concave bank upstream. This mechanism would explain why the radiocarbon ages of the two southernmost radiocarbon samples cover the same period (64–213 versus 69–214 CE; Fig. 4 and Table 2): they probably derived from the same sedimentary stock further upstream.

Waste deposition in the palaeochannel

The ancient palaeochannel and the way it developed allowed for the accumulation of a fluvial sedimentary stock at a depth of 2 to 3.5 m. This remained below the water table in apparently stable hydromorphic conditions and so enabled the good preservation of carpological and palynological material that complements the archaeozoological and anthracological assemblages.[23]

The archaeozoological assemblage is dominated by the remains of livestock (cattle, pigs, sheep, and goats) as well as other domestic species (chickens, equines, and dogs). Traces of carcass cuttings, particularly the chopping of animal legs into pieces, are suggestive of butchery and consumption of meat. The assemblage also includes some bone remains that show no traces of human intervention, likely from wild species (lagomorphs, murids) and species whose domestic or wild status remains undetermined (cats, small canids, Columbidae). Most of the fragments have been rolled and the bone surfaces are disintegrating (desquamation), indicating their displacement by the watercourse before their final deposition. Traces of trimming indicate the intervention of detrivores on some bones. The archaeozoological assemblage is therefore not in a primary position and demonstrates diversified inputs via the Vistre de la Fontaine River.

The carpological assemblage is diversified, composed of cultivated taxa, crop weeds, woodland, forest, and forest borders. The anthropic contribution can be seen in the high proportion of fruit and seed remains that may have been of nutritional benefit (figs, grapes, cherries/wild cherries, olives, possibly pomegranates, melons/cucumbers, gourds, parsnip, and coriander seeds), as well as in the high level of fragmentation of some remains, indicating hulling or grinding. The discovery of some 40 rolled and highly eroded remains that resemble either shell (nuts?) or pit (olives, *Prunus* family?) fragments is suggestive of a contribution of allochthonous material, probably from the ancient city of Nîmes. Roman-period sites inside and outside the city walls yielded similar "economic" taxa to those found on the Vistre de la Fontaine 2-2 site, and these are common in urban and periurban settlements and in funerary environments.[24] The Vistre de la Fontaine exported some of its organic waste outside of the town. On the other hand, the discovery of pressed

[23] Scrinzi et al. 2021.

[24] Tillier 2019.

Fig. 4 - Colour online, B/W in print

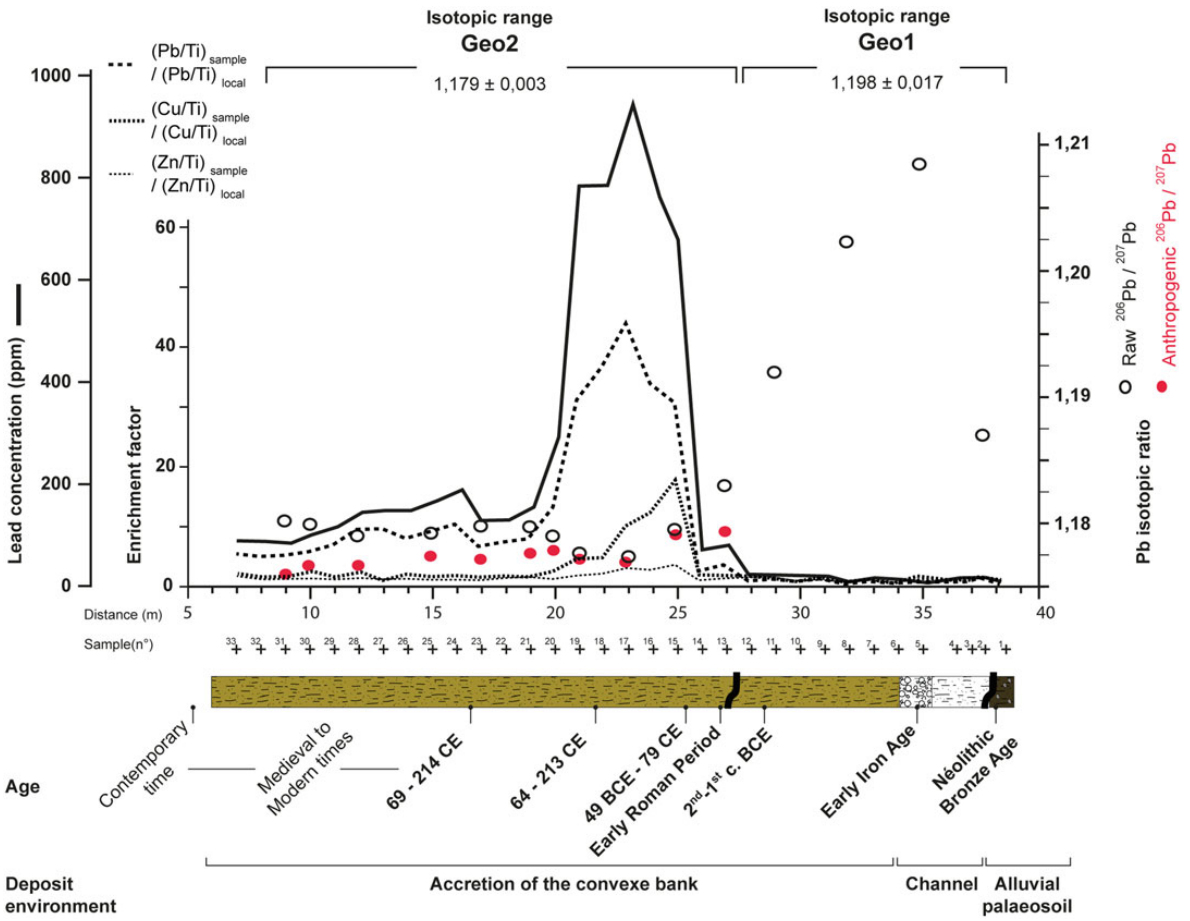

Fig. 4. *Synthetic stratigraphic log of the site showing chronology, Pb concentration (ppm), Pb, Cu, and Zn enrichment factors (calculated according to Barbieri 2016), and $^{206}Pb/^{207}Pb$ isotopic ratios, raw and in excess (Pb of anthropic origin). Lead isotope ratios are associated with an error bar lower than 0.012%. (C. Flaux.)*

grape residues (highly fragmented pips, pedicels, skin, stalk, and aborted berries) indicates there was no displacement in the watercourse or local discharge either from the banks of the channel or directly from the bridge that overhangs the deposition area. In an urban or rural context, the Vistre de la Fontaine resembles a waste disposal area.

The anthracological and xylological samples collected in the Vistre de la Fontaine palaeochannel are also very diverse, including soaked fragments from timber, charcoal of fruit and ornamental taxa, and fuelwood. The high proportion of heather within the anthracological spectrum, which has been shown to be a fuel of choice of the ancient city,[25] indicates that the assemblage is, at least in part, representative of the range of waste that passed from the city of Nîmes into the riverbed. Charcoal and soaked-wood analysis shows that the zones used for gathering firewood or for the manufacture of shaped objects include all the wooded environments present around Nîmes: the mixed oak forest of the Garrigues and Costières, the alluvial forest of the plain, the riparian forest, the possible relict woodlands on nearby mountains, and also cultivated trees. This diversity reflects the wider environment of Nîmes rather than just the immediate riparian setting of the site being studied.

[25] Figueiral et al. 2017.

In antiquity, the demographic and urban expansion of Nemausus, as well as the development of cottage industries and commercial trade, led to a proliferation of waste and various kinds of pollution. Recent studies of ancient rubbish tips indicate a concern to preserve the cleanliness of public areas and efforts to relocate rubbish dumps to the periphery of the Augustan enclosure and to roadside locations.[26] Bioarchaeological remains found in the Roman channel of the Vistre de la Fontaine underline the fact that the river also transported urban waste outside the city of Nîmes, suggesting that the river acted as a sewer. Archaeological research in Nîmes has shown that the Vistre de la Fontaine was indeed largely integrated into extended and complex wastewater drainage networks.[27] The Arles harbor dump in the Rhône is representative in this respect, since it gathered thousands of waste items from the city's domestic, cottage-industry, and harbor activities.[28] In Nîmes, the urban river also carried invisible waste such as metals.

Chemical imprint

Lead contamination of the banks

The overall macroscopic homogeneity of the sedimentary matrix of the accretionary sequence of the Vistre de la Fontaine's convex palaeobank, as expressed by grain size data, is confirmed by the weak variation of the calcium, potassium, and iron content (Fig. 3 and Table 1) that dominate the elemental composition of the detrital load. This homogeneity contrasts with the variability of Pb content (Fig. 3). In the north–south direction of the lateral accretion of the palaeo-Vistre de la Fontaine's convex bank, the Pb profile shows an initially low content (10–20 ppm), followed by a sharp rise to nearly 1,000 ppm, and a fall to rather steady concentrations (100—200 ppm) that remain about ten times higher than the geochemical background recorded at the beginning of the sequence, that is, the Neolithic soil. Copper (Cu) and zinc (Zn) levels broadly follow a similar pattern (Fig. 3).

Metal enrichment factors (EF_m with m = Pb, Cu, or Zn) were calculated to estimate the metal enrichment in relation to the local geochemical background:

$$EF_m = \left(m/Ti\right)_{sample} / \left(m/Ti\right)_{local\ geochemical\ background}.$$[29]

The metal concentration is normalized to titanium (Ti), which is a conservative terrigenous element in soils,[30] that is, not prone to mobility, with a variability linked to that of the natural source from which the sediments are derived. The local geochemical background corresponds to the metal content measured within pre-anthropic sediments from samples 3, 4, and 6 to 11 (Fig. 3) because these sediments have a silicoclastic and silty matrix like contaminated sediments. An EF_m >3 is considered enough to suggest excess accumulated metal that may be of anthropogenic origin.[31] EF values above 40 are considered extremely high.[32] These enrichment factors are shown in Figure 4, where a significant enrichment is

[26] Monteil et al. 2003; Le-roy et al. 2019.

[27] Veyrac 2006

[28] Djaoui dir. 2019.

[29] Calculated according to Barbieri 2016.

[30] e.g., Shotyk et al. 2002.

[31] Véron et al. 2006; Delile 2014.

[32] Barbieri 2016.

evidenced during the Early Roman Empire (20–25m in the sequence) for Pb (EF_{Pb} max = 44), to a lesser extent for Cu (EF_{Cu} max = 18), and slightly above the materiality threshold for Zn (EF_{Zn} max = 3.5). EF_{Pb} indicates a massive and sudden source of lead input into the alluvial sedimentary system of the Vistre de la Fontaine. For comparison, an environmental lead contamination during the Roman Empire was also observed in the Étang de Thau by elemental and isotopic analyses of mussel shell.[33]

Possible source of Pb contamination

Although ceramic or wooden pipes existed during antiquity, the use of Pb pipes was very common in Roman times,[34] this material being known for its elasticity and resistance to pressure.[35] In Nîmes, A. Pelet described in 1863 "an infinite number of lead pipes criss-crossing our city [Nîmes] which we discover every day buried under our soil."[36] In particular, the sector of the Fontaine spring has yielded Pb pipes in abundance, as has the Castellum sector, the sewer and distributor of water from the Nîmes aqueduct. The geography of the lead pipe discoveries (40 in Alain Veyrac's catalogue),[37] the ten leakage pipes from the Castellum, each about 35 cm in diameter, and the distribution of the thermal baths in the city provide, inter alia, evidence that almost the entire extent of the Roman city was supplied with water by two distinct networks independent of each other (the aqueduct of Nîmes and the conveyance of water from the Fontaine source), composed mainly of Pb pipes. The ancient main sewers were drained away in the main water flow, downstream of the Vistre de la Fontaine.[38] Therefore, the discharge of bioarchaeological remains (partly resulting from domestic and cottage-industry discharges from Nîmes) and Pb contaminants downstream of the Roman city is no wonder. The Pb anomaly starts abruptly after the construction of the bridge during the Early Roman Empire. The archaeological data from Nîmes show that the upkeep of the Roman and public water management system declined during the 2nd c. CE and ceased during the 4th c. CE.[39] Our hypothesis is that the Pb peak identified in the sediments of the convex bank of a meander of the Vistre de la Fontaine evidences the installation, use, and then abandonment of Nîmes's lead pipe network during the Early Roman Empire. Comparing the isotopic signature of these remains with that of the contamination generated in the river will allow the validity of this hypothesis to be examined.

Origin of Pb ore

Alain Veyrac assumed that Pb pipe manufacturing workshops must have existed in Nîmes, at least to satisfy local demand.[40] This hypothesis was confirmed by the discovery of two Pb pipes in the vicinity of Nîmes, at Balaruc-les-Bains (Hérault), each bearing an

33 Labonne et al. 1998.
34 Nriagu 1983.
35 Veyrac 2006, 162-177.
36 Veyrac 2006, 169.
37 Veyrac 2006
38 Monteil 1999; Veyrac 2006
39 Monteil 1999.
40 Veyrac 2006.

inscription referring to the Nîmes colony.[41] Likewise, in the Ambrussum way station in Villetelle (Hérault), a stamp on a Pb pipe showed similarities to the onomastics of the city of Nîmes, suggesting a plumbing company based in Nîmes may have been involved.[42] Using stable Pb isotopes, we may infer the geographic origin of the Pb ores that contaminated the palaeochannel during the Roman Empire.

The excess Pb measured in the sediments of the banks of the Vistre de la Fontaine provides evidence of an anthropogenic contribution superimposed on the local geochemical background. Both may be identified by their isotopic signatures. The horizontal profile of the $^{206}Pb/^{207}Pb$ ratio of the alluvial sequence is characterized by two main isotopic fields, Geo1 and Geo2 (Fig. 4). The Geo1 field, associated with relatively low Pb content (9–25 ppm), has a variable and more radiogenic isotopic signature ($^{206}Pb/^{207}Pb = 1.198 \pm 0.017$), as compared to the Geo2 field, which is characterized by higher Pb content (100–1,000 ppm) and a more homogeneous and less radiogenic isotopic signature ($^{206}Pb/^{207}Pb = 1.179 \pm 0.003$). The most radiogenic values are consistent with those of uncontaminated sediments deposited in the western Mediterranean basin[43] ([Pb] = 13–20 ppm; $^{206}Pb/^{207}Pb = 1.195$–$1.233$); in the ancient harbor of Fréjus[44] ([Pb] = 14–20 ppm; $^{206}Pb/^{207}Pb = 1.202 \pm 0.002$); and in the uncontaminated sediments of the Étang de Thau, southwest of Montpellier[45] ($^{206}Pb/^{207}Pb = 1.200 \pm 0.003$). Within the Geo1 field, samples 2 and 11 show a slightly less radiogenic isotope ratio ($^{206}Pb/^{207}Pb$ around 1.19), which could indicate differentiated (anthropogenic?) Pb contributions prior to the Roman-period contamination. We believe that the Geo1 isotopic field constitutes, if not the natural geochemical background given an unstable isotopic signature from possible low amplitude proto-contamination sources, at least the local geochemical background before the advent of the Roman Empire. Given the relative uniformity of the measured $^{206}Pb/^{207}Pb$ ratios from each Geo field, the mean isotopic signature of the excess Pb in the Roman palaeo-bank can be assessed from the $^{206}Pb/^{207}Pb$ (y) vs. 1/Pb (x) relationship (Fig. 5C). The latter shows a significant strong correlation ($r^2 = 0.97$, $p < 0.01$) with $y = 1.178 + 0.3x$. Therefore, one can calculate that the mean isotopic imprint of Pb in excess into the fluvial sedimentary system of the Vistre de la Fontaine during the Roman Empire is $^{206}Pb/^{207}Pb = 1.178 \pm 0.002$, much less radiogenic than the local geochemical background (student *t*-test, $p < 0.05$). The Pb isotope imprint introduced in excess (R_{Xs}) into the environment from this period can also be calculated by the following isotopic mixing equation (with R: isotopic ratio and Pb: lead content):

$$R_{raw} * Pb_{raw} = R_{Xs} * Pb_{Xs} + R_{local} * Pb_{local}.$$

The term "raw" is measured in the sample. The term "local" corresponds to the five samples of the sequence with the lowest lead content (considered as carrying the local geochemical background; samples 2, 5, 7, 8, and 11). Pb_{Xs} (Pb in excess) = Pb_{raw} - Pb_{local}. The mean calculated isotope signature of excess Pb (1.179 ± 0.002) is similar to that determined from Figure 5, as expected from the remarkably constant Pb_{Xs} isotope imprint during the

41 Veyrac 2006, 173, fig. 95.

42 Fiches and Rebière 2010, 327.

43 Ferrand et al. 1999.

44 Véron et al. 2018.

45 Monna et al. 2000.

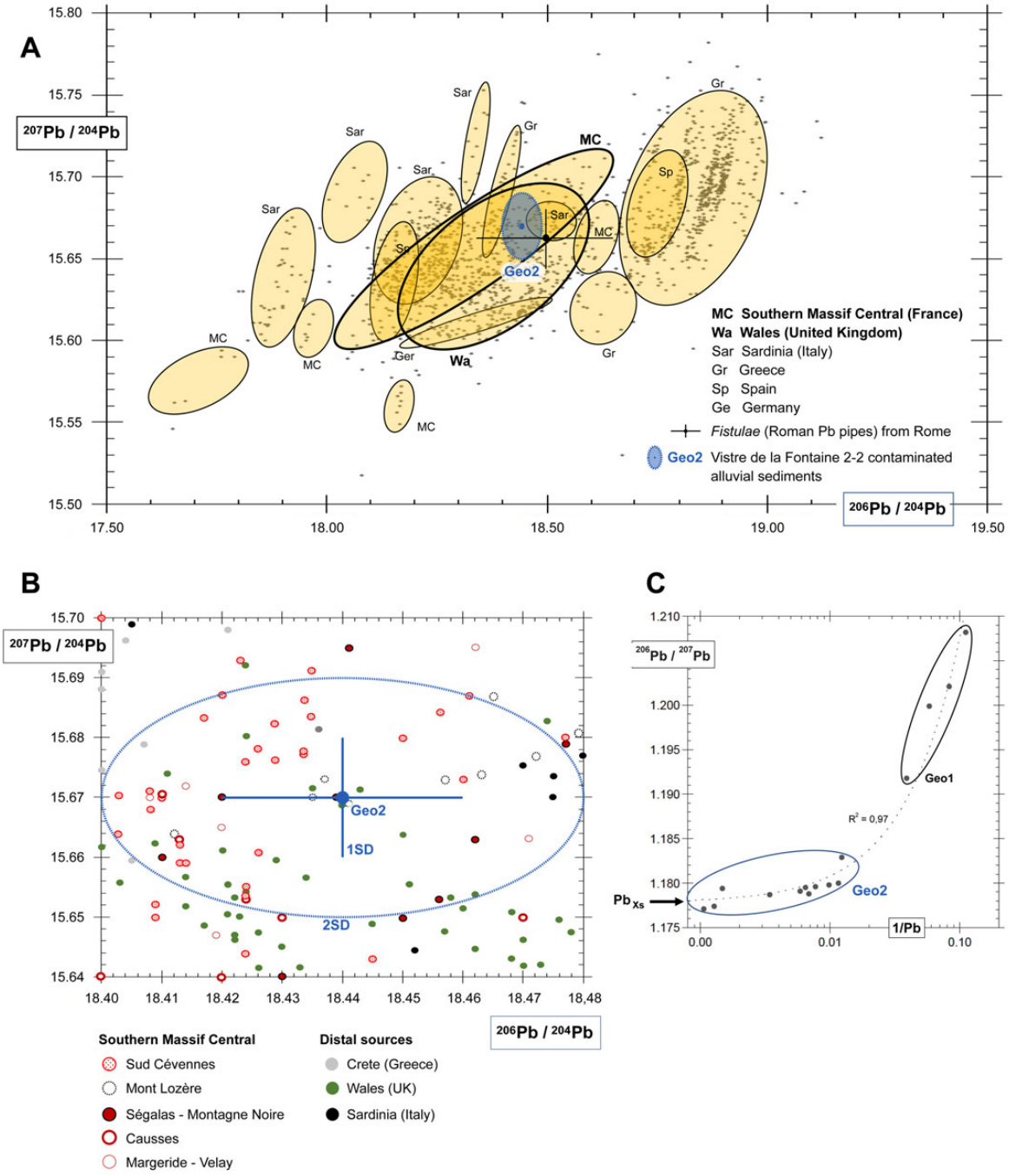

Fig. 5 - Colour online, B/W in print

Fig. 5. ***A- and B-*** *$^{206}Pb/^{204}Pb$ vs. $^{207}Pb/^{204}Pb$ of known lead ores that can fit the Geo2 isotopic imprint (Arribas and Tosdal 1994; Barnes* et al. *1974; Brevart* et al. *1982; Pomiès* et al. *1988; Ruiz* et al. *2002; Craddock* et al. *1985; Hunt-Ortiz 2003; Krahn and Baumann 1996; Le Guen and Lancelot 1989; Le Guen* et al. *1991; Leach* et al. *2001; Leach* et al. *2006; Marcoux 1986; Marcoux and Brill 1986; Niederschlag* et al. *2003; Rohl 1996; Rosman* et al. *1997; Sangster* et al. *2000; Stos-Gale* et al. *1995; Stos-Gale* et al. *1996; Stos-Gale and Gale 2009; Swainbank* et al. *1982; Wagner* et al. *1979. ~~Calibration carried out according to Reimer~~* et al. *~~2020~~). Geo2 is the mean calculated isotopic signature of lead in excess during the Roman Empire sequence ("SD" = standard deviation).* ***C-*** *Determination of the excess Pb isotopic imprint from the linearity between Geo1 and Geo2 fields. (C. Flaux.)*

Roman sequence and beyond. This isotopic composition has been compared to a compilation of the isotopic signatures of lead deposits located in massifs where ancient works have been identified. The $^{206}Pb/^{204}Pb$ and $^{207}Pb/^{204}Pb$ Pb_{Xs} signatures of the Geo2 field

are used owing to the discrimination ability of the normalization to the non-radiogenic ^{204}Pb isotope.[46] These Pb_{Xs} isotopic ratios are calculated using the mixing equation. The different geographical provenances compose broad, sometimes scattered, and frequently overlapping isotopic domains, indicating isotopic heterogeneity of the ores (Fig. 5A). A closer analysis of $^{206}Pb/^{204}Pb$ vs. $^{207}Pb/^{204}Pb$ ratios of excess Pb reveals two possible regional sources within the uncertainty range of the Nîmes footprint (Fig. 5B): Great Britain (Northumberland, Devon, Staffordshire, and Gwynedd) and the southern Massif Central (Mont Lozère, Ségalas-Montagne Noire, southern Cévennes). The latter signature highlights the systematic prospecting of Cu-Pb-Ag deposits in the Montagne Noire during antiquity[47] and could confirm the southern Massif Central as a potential Pb-Ag mining region during the Roman period,[48] more firmly evidenced for the Middle Ages in metallurgical works and environmental deposits.[49] Alternatively, practices of salvaging and recycling implemented by the Romans[50] may have produced a mixture from several original sources that would be precluded from identification. Interestingly, the Pb_{Xs} isotopic imprint recorded in Vistre de la Fontaine 2-2 Roman sediments is similar to that of ancient Roman lead pipes from Rome (Fig. 5A).[51]

Lead isotope analysis also makes clear that this Roman-period contamination has been perpetuated until the modern era, most probably due to a remobilization of the "ancient reservoir," which would have been redistributed by the alluvial dynamics along the meandering longitudinal profile of the Vistre de la Fontaine. As such, the excess Pb introduced at a given time into a fluvial environment could remain a passive source of contamination of local sediments for several thousand years, Pb being relatively stable in soils due to its insolubility in clean water[52] and its resistance to leaching.[53] Such pervasive Roman Pb pollution in modern fluvial sediments has also been identified in the Tiber delta.[54]

Conclusion

This study illustrates the riverine transport of diversified anthropogenic waste from the city of Nîmes towards its rural periphery since the Early Roman Empire, at a location 3 km downstream of the urban center, including remains from butchery, consumption of fruit, and combustion. These results confirm the role played by watercourses in evacuation of urban waste from ancient cities.[55] The human imprint is also characterized by heavy metal (Pb, Cu, and Zn) accumulation onto deposited sediment particles. It is likely that the Pb peak mirrors the expansion and retraction of the Nemausus water supply system during the Early Roman Empire. The Vistre de la Fontaine, originating from a sacred

46 Doe, 1970.

47 Mantenant 2014; Mantenant and Munoz 2017.

48 Le Roux et al. 2005; Delile et al. 2014; Delile et al. 2016; Hanel and Bode, 2016; Delile et al. 2017; Parjanadze and Bode, 2017; Rothenhöfer et al., 2017; McConnell et al. 2018; Bode et al. 2018.

49 Baron et al. 2005; Baron et al. 2006; Baron et al. 2009.

50 Delile et al. 2017.

51 Delile et al. 2014, 2017.

52 Lovering 1976.

53 Du Laing et al. 2009.

54 Delile et al. 2014.

55 Dupré Raventós and Remolà Vallverdù 2000.

spring dedicated to the eponymous god of the city, Nemausus, became a sewer downstream and a vector, from the Roman city to the countryside, of visible and invisible waste. It has generated significant metallic palaeocontamination in the sediments of the convex bank of a meander of the river.

The perception of lead contamination remains topical: in the Nîmes area, little is known of the concentration of heavy metals in present-day watercourses.[56] The Vistre de la Fontaine 2-2 site shows that their presence may be a distant legacy, with local levels of long-lasting ancient Pb higher than the values for an impact on human health (sensitive Pb environmental impact value VCI of 400 ppm)[57] and well above the WHO/FAO permissible limit of 50 ppm.[58] Stable Pb isotopes show not only the possible geographic origin of Pb ores imported into the city of Nîmes during the Roman Empire (from the southern French Massif Central and/or Great Britain) but also the reworking of this ancient contamination into posterior alluvial deposits. This site shows that local present-day heavy metal anomalies may be inherited from industrial activities that date back to Roman Antiquity.

Acknowledgments: We thank three anonymous reviewers and the editor whose insightful comments helped improve the manuscript. We are grateful to Mélanie Errera, Loriane Besombes, and Florient Ortis for their great help during fieldwork. We also thank Christophe Pellecuer, chief curator of heritage of the French ministry of culture and communication, who fully promoted this study beyond its initial archaeological prescription. The study was supported by APIC 2021 funding from CEREGE. We thank Hélène Mariot for their careful maintenance of CEREGE's clean laboratory. The CEREGE group was supported by the French Investissement d'Avenir program through the Equipex ASTER-CEREGE.

Competing interests: The authors declare none.

References

Arribas, A., and R. M. Tosdal. 1994. "Isotopic composition of Pb in ore deposits of the Betic Cordillera, Spain: Origin and relationship to other European deposits." *Economic Geology* 89, no. 5: 1074–93.

Barbieri, M. 2016. "The importance of enrichment factor (EF) and geoaccumulation index (Igeo) to evaluate the soil contamination." *Journal of Geology & Geophysics* 5, no. 1: 1000237.

Barnes, I. L., W. R. Shields, T. J. Murphy, and R. H. Brill. 1974. "Isotopic analysis of Laurion lead ores." In *Archaeological Chemistry,* ed. C. W. Beck, 1–10. Washington: American Chemical Society.

Baron, S., M. Lavoie, A. Ploquin, J. Carignan, M. Pulido, and J.-L. De Beaulieu. 2005. "Record of metal workshops in peat deposits: History and environmental impact on the Mont Lozère Massif, France." *Environmental Science and Technology* 39, no. 14: 5131–40.

Baron, S., J. Carignan, S. Laurent, and A. Ploquin. 2006. "Medieval lead making on Mont-Lozère Massif (Cévennes-France): Tracing ore sources by using Pb isotopes." *Applied Geochemistry* 21: 241–52.

Baron, S., C. Le Carlier, J. Carignan, and A. Ploquin. 2009. "Archaeological reconstruction of medieval lead production: Implications for ancient metal provenance studies and paleopollution tracing by Pb isotopes." *Applied Geochemistry* 24: 2093–101.

Bode, M., P. Rothenhöfer, and D. G. Batanero. 2018. "Lost in the south: A Roman copper ingot from the area of Tarragona in the Baetica." *Revista Onoba* 6: 243–48.

---

56 PAGD, 2020.

57 Laperche et al. 2004, 109.

58 WHO/FAO 2001; de Vries et al. 2003.

Breuil, J.-Y., and B. Houix, eds. 2017. *L'histoire d'un quartier de Nemausus, Nîmes – Parking Jean-Jaurès*. Nîmes: INRAP Méditerranée.

Brevart, O., B. Dupre, and C. J. Allegre. 1982. "Metallogenic provinces and the re- mobilization process studied by lead isotopes; lead-zinc ore deposits from the southern Massif Central, France." *Economic Geology* 77: 564–75.

Cayn, P., ed. 2016. *Cadereau du Valladas, tronçon Aérodrome-Miremand, Lot 1 (Nîmes, Languedoc-Roussillon, Gard)*. Nîmes: INRAP Méditerranée.

Chevillot, P., P. Séjalon, and J.-Y. De Breuil. 2008. "L'approche géomorphologique systématique à l'échelle d'un territoire : le cas de Nîmes." *Les Cahiers de l'Inrap* 2: 1–8.

Chevillot, P., S. Martin, J.-Y. Breuil, H. Pomaredes, and P. Sejalon. 2010. "Mobilités et héritages dans la plaine de Nîmes (Gard, France). Regards croisés sur l'occupation humaine à l'Holocène." *Quaternaire* 21: 459–74.

Craddock, P. T., I. C. Freestone, N. H. Gale, N. D. Meeks, B. Rothenberg, and M. S. Tite. 1985. "The investigation of a small heap of silver smelting debris from Rio Tinto, Huelva." In *Furnaces and Smelting Technology in Antiquity*, ed. P. T. Craddock and M. J. Hughes, 199–217. London: British Museum.

de Vries, W., G. Schütze, S. Lots, M. Meili, P. Römkens, L. de Temmerman, and M. Jakubowski. 2003. "Critical limits for cadmium, lead and mercury related to ecotoxicological effects on soil organisms, aquatic organisms, plants, animals and humans." In *Proceedings of the Expert Meeting on Critical Limits for Heavy metals and Methods for their Application*, ed. G. Schütze, U. Lorent, and T. Spranger, 29–78. Berlin: Umweltbundesamt.

Delile, H. 2014. *Signatures des paléo-pollutions et des paléoenvironnements dans les archives sédimentaires des ports antiques de Rome et d'Éphèse*. PhD diss., Univ. Lumière Lyon 2.

Delile, H., J. Blichert-Toft, J.-P. Goiran, S. Keay, and F. Albarède. 2014. "Lead in ancient Rome's city waters." *Proceedings of the National Academy of Sciences* 111, no. 18: 6594–99.

Delile H., J. Blichert-Toft, J.-P. Goiran, F. Stock, F. Arnaud-Godet, J.-P. Bravard, H. Brückner, and F. Albarède. 2015. "Demise of a harbor: A geochemical chronicle from Ephesus." *JAS* 53: 202–13.

Delile H., D. Keenan-Jones, J. Blichert-Toft, J.-P. Goiran, F. Arnaud-Godet, P. Romano, and F. Albarède. 2016. "A lead isotope perspective on urban development in ancient Naples." *Proceedings of the National Academy of Sciences* 113, no. 22: 6148–53.

Delile H., D. Keenan-Jones, J. Blichert-Toft, J.-P. Goiran, F. Arnaud-Godet, and F. Albarede. 2017. "Rome's urban history inferred from Pb-contaminated waters trapped in its ancient harbor basins." *Proceedings of the National Academy of Sciences* 114, no. 38: 10059–64.

Delile H., E. Pleuger, J. Blichert-Toft, and A. I. Wilson. 2019. "Economic resilience of Carthage during the Punic Wars: Insights from sediments of the Medjerda delta around Utica (Tunisia)." *Proceedings of the National Academy of Sciences* 116, no. 20: 9764–69.

Djaoui, D., ed. 2019. "Difficultés et intérêts à étudier un contexte portuaire fluviomaritime en zone périurbaine (50-14 apr. J.-C.)." In *De la Gaule à l'Orient Méditerranéen. Fonctions et statuts des mobiliers archéologiques dans leur contexte*, ed. P. Ballet, S. Lemaître, and I. Bertrand, 245–57. Rennes: Presses Universitaires de Rennes.

Doe, B. R. 1970. *Lead Isotopes*. Berlin: Springer Verlag.

Doucelance, R., and G. Manhès. 2001. "Reevaluation of precise lead isotope measurements by thermal ionization mass spectrometry: Comparison with determinations by plasma source spectrometry." *Chemical Geology* 176: 361–77.

Du Laing, G., J. Rinklebe, B. Vandecasteele, E. Meers, and F. M. G. Tack. 2009. "Trace metal behaviour in estuarine and riverine floodplain soils and sediments: A review." *Science of The Total Environment* 407, no. 13: 3972–85.

Dupré Raventos, X., and J. A. Remolà Vallverdù. 2000. *Sordes urbis: la eliminación de residuos en la ciudad romana*. Roma: Bibliotheca italica 24.

Elmaleh, A., A. Galy, T. Allard, R. Dairon, J. A. Day, F. Michel, N. Marriner, C. Morhange, and F. Couffignal. 2012. "Anthropogenic accumulation of metals and metalloids in carbonate-rich sediments: Insights from the ancient harbor setting of Tyre (Lebanon)." *Geochimica et Cosmochimica Acta* 82: 23–38.

Fabre, G., and M. Monteil. 2011. "Urbanisation antique, hydrogéomorphologie et impacts postérieurs sur le site de Piémont de Nîmes." In *Temps de l'eau. Sites et monuments entre Vidourle et Rhône*, ed. G. Fabre, 5–10. Nîmes: Bulletin de l'École Antique de Nîmes.

Fagel, N., M. Lechenault, F. Fontaine, E. Pleuger, J. Otten, M. Allan, M. Ghilardi, N. Mattielli, and J.-P. Goiran. 2017. "Record of human activities in the Pb isotopes signatures of coastal sediments from the Roman archaeological site of Cala Francese, Cape Corsica (France)." *JAS: Reports* 12: 770–81.

Ferrand, J. L., B. Hamelin, and A. Monaco. 1999. "Isotopic tracing of anthropogenic Pb inventories and sedimentary fluxes in the Gulf of Lions (NW Mediterranean sea)." *Continental Shelf Research* 19, no. 1: 23–47.

Fiches, J. L., and J. Rebière. 2010. "Caisson décoré et tuyaux de plomb découverts à *Ambrussum*: questions d'adduction d'eau dans l'agglomération routière." *Revue Archéologique de Narbonnaise* 43, no. 1: 313–30.

Figueiral, I., S. Ivorra, J.-Y. Breuil, V. Bel, and B. Houix. 2017. "Gallo-Roman Nîmes (southern France): A case study on firewood supplies for urban and proto-urban centers (1st B. C.-3rd A. D.)." *Quaternary* 458: 103–12.

Flaux, C., M. Scrinzi, and H. Djerbi. 2022. "À quand remonte l'état de référence 'naturel' du Vistre de la Fontaine (Nîmes)?" *Méditerranée* [Online], Paleoenvironment, Geoarchaeology, Historical Geography. http://journals.openedition.org/mediterranee/12628.

Gelly, R., Z. Fekiacova, A. Guihou, E. Doelsch, P. Deschamps, and C. Keller. 2019. "Lead, zinc, and copper redistributions in soils along a deposition gradient from emissions of a Pb-Ag smelter decommissioned 100 years ago." *Science of The Total Environment* 665: 502–12.

Hanel, N., and M. Bode. 2016. "Messingbarren aus einem römischen Schiffswrack bei Aléria (Korsika)." In *From Bright Ores to Shiny Metals. Festschrift for Andreas Hauptmann on the Occasion of 40 Years Research in Archaeometallurgy and Archaeometry*, ed. G. Körlin, M. Prange, Th. Stöllner, and Ü. Yalçin, 167–81. Bochum: Der Anschnitt.

Hong, S., J.-P. Candelone, C. C Patterson and C. F. Boutron. 1994. "Greenland ice evidence of hemispheric lead pollution two millennia ago by Greek and Roman civilizations." *Science* 265, no. 5180: 1841–43.

Hunt-Ortiz, M. A. 2003. *Prehistoric Mining and Metallurgy in South-West Iberian Peninsula*. BAR International Series 1188. Oxford: British Archaeological Reports.

Jallet, F., S. Barberan, P. Chevillot, D. Colonge, V. Forest, V. Mourre, S. Négroni, C. Pallier, R. Pellé, A. Ratsimbas, P. Séjalon, L. Duflot, A. Farge, F. Robin, and H. Vergély, eds. 2017. *Vistre de la Fontaine 2 – Tranche 1 (Occitanie, Gard, Nîmes)*. Nîmes: INRAP Méditerranée.

Kilbride, C., J. Poole, and T.-R. Hutchings. 2006. "A comparison of Cu, Pb, As, Cd, Zn, Fe, Ni, and Mn determined by acid extraction/ICP-OES and ex situ field portable X-ray fluorescence analyses." *Environmental Pollution* 143, no. 1: 16–23.

Krahn, L., and A. Baumann. 1996. "Lead isotope systematics of epigenetic lead-zinc mineralization in the western part of the Rheinisches Schiefergebirge, Germany." *Mineralium Deposita* 31, no. 3: 225–37.

Labonne, M., D. Ben Othman, and J.-M. Luck. 1998. "Recent and past anthropogenic impact on a Mediterranean lagoon: Lead isotope constraints from mussel shells." *Applied Geochemistry* 13, no. 7: 885–92.

Laperche V., M. C. Dictor, B. Clozel-Leloup, and P. Baranger. 2004. *Guide méthodique du plomb appliqué à la gestion des sites et des sols pollués*. Orléans: BRGM.

Le Guen, M., and J. Lancelot. 1989. "Origine du Pb-Zn des minéralisations du Bathonien sud-cévenol. Apport de la géochimie isotopique comparée du plomb des galènes, de leur encaissant et du socle." *Chronique de la recherche minière* 495: 31–36.

Le Guen, M., J. J. Orgeval, and J. Lancelot. 1991. "Lead isotopic behavior in a polyphase Pb-Zn ore deposit, Les Malines (Cévennes, France)." *Mineralium Deposita* 26, no. 3: 180–88.

Le Roux, G., A. Véron, and C. Morhange. 2003. "Geochemical evidences of early anthropogenic activity in harbour sediments from Sidon." *Archaeology and History in Lebanon* 18: 115–19.

Le Roux, G., A. Véron, and C. Morhange. 2005. "Lead pollution in the ancient harbours of Marseilles." In "Environnements littoraux méditerranées, héritages et mobilité," Special edition, *Méditerrannée* 104, nos. 1–2: 31–35.

Le-Roy, L., M. Couval, M. Scrinzi, S. Aspord-Mercier, B. Favennec, A. Renaud, A. Malignas, M. Gagnol, O. Mignot, J. Pech, Y. Zaaraoui, T. Canillos, N. Clément, and A. Garnotel. 2019. *Le Jardin du Musée de la Romanité. Saint-Joseph – Musée de la Romanité – 2. Nîmes, Gard (30)*. Cournonterral: Mosaïques Archéologie.

Leach, D. L., W. Premo, M. Lewchuk, B. Henry, M. Le Goff, H. Rouvier, J. C. Macquar, and J. Thibieroz. 2001. "Evidence for Mississippi valley-type lead–zinc mineralization in the Cévennes region, southern France, during Pyrenees Orogeny." In *Mineral Deposits at the Beginning of the 21st* Century, ed. A. Piestrzynski, 157–60. Lisse: Swets and Zeitlinger.

Leach, D., J. C. Macquar, V. Lagneau, J. Leventhal, P. Emsbo, W. Premo. 2006. "Precipitation of lead-zinc ores in the Mississipi Valley-type deposit at Trèves, Cévennes region of southern France." *Geofluids* 6: 24–44.

Lovering, T. G., ed. 1976. *Lead in the Environment*. Washington: US Geological survey professional paper 957.

Manhès, G., J. F. Minster, C. J. Allègre. 1978. "Comparative uranium-thorium-lead and study of the Saint Sèverin amphoterite: Consequences for early solar system chronology." *Earth and Planetary Science Letters* 39, no. 1: 14–24.

Mantenant, J. 2014. *Montagnes métallifères de Gaule méditerranéenne. Approche archéologique et historique de la production des métaux en Languedoc occidental du début du second âge du Fer à la fin de la période romaine (IVème s. av. n. è. – Vème s. de n. è.)*. PhD diss., Univ Toulouse-Le Mirail.

Mantenant, J., and M. Munoz. 2017. "L'exploitation des gisements non-ferreux des Pyrénées de l'Est aux trois derniers siècles avant notre ère: une ruée vers l'argent? Le cas des Corbières." *Treballs d'Arqueologia* 21: 149–79.

Marcoux, E. 1986. *Isotopes du plomb et paragenèses métalliques, traceurs de l'histoire des gites minéraux. Illustration des concepts de source, d'héritage et de régionalisme dans les gites francais, applications en recherche minière*. PhD thesis, Univ. Clermont-Ferrand.

Marcoux, E., and H. Brill. 1986. "Héritage et sources des métaux d'après la géochimie isotopique du plomb. Exemple des minéralisations filoniennes (Sb, Pb, Ba, F) du Haut-Allier (Massif Central, France)." *Mineral Deposita* 21, no. 1: 35–43.

Maréchal, J.-C., V. Petit, and B. Ladouche. 2004. *Synthèse des connaissances géologiques et hydrogéologiques sur le bassin d'alimentation de la Fontaine de Nîmes*. Orléans: BRGM.

McConnell, J. R., A.I. Wilson, A. Stohl, M. M. Arienzo, N.J. Chellmann, S. Eckhardt, E. M. Thompson, A.M. Pollard, and J. P. Steffensen. 2018. "Lead pollution recorded in Greenland ice indicates European emissions tracked plagues, wars, and imperial expansion during antiquity." *Proceedings of the National Academic Science* 115, no. 22: 5726–31.

Ménillet, F., and H. Paloc. 1973. *Notice de la carte géologique de Nîmes au 1/50 000*. Orléans: BRGM.

Monna, F., N. Clauer, T. Toulkeridis, and J.R. Lancelot. 2000. "Influence of anthropogenic activity on the lead isotope signature of Thau Lake sediments (southern France) : origin and temporal evolution." *Applied Geochemistry* 15, no. 9: 1291–305.

Monteil, M. 1999. *Nîmes antique et sa proche campagne. Étude de topographie urbaine et périurbaine (fin VIe s. av. J.-C. – VIe s. apr. J.-C.)*. Lattes : Monographies d'archéologie méditerranéenne 3.

Monteil, M., S. Barberan, V. Bel, and M.-L. Hervé. 2003. "Dépotoirs domestiques et déchets artisanaux : l'exemple de Nîmes (Gard) au Haut-Empire." In *La ville et ses déchets dans le monde romain : rebuts et recyclages*, ed. P. Ballet, P. Cordier, and N. Dieudonné-Glad, 121–31. Montagnac: Monique Mergoil.

Niederschlag, E., E. Pernicka, Th. Seifert, and M. Bartel-Heim. 2003. "The determination of lead isotope ratios by multiple collector ICP-MS: A case study of early bronze age artifacts and their possible relation with ore deposits of the Erzgebirge." *Archaeometry* 45, no. 1: 61–100.

Nin, N., and M. Leguilloux. 2003. "La gestion des déchets à Aix-en-Provence dans l'Antiquité." In *La ville et ses déchets dans le monde romain : rebuts et recyclages*, ed. P. Ballet, P. Cordier, and N. Dieudonné-Glad, 133–64. Montagnac: Monique Mergoil.

Nriagu, J. O. 1983. *Lead and Lead Poisoning in Antiquity*. Hoboken: John Wiley.

PAGD. 2020. *Plan d'Aménagement et de Gestion Durable (PAGD) des ressources en eau et des milieux aquatiques & Règlement*. Caissargues: ETPB Vistre-Vistrenque.

Parjanadze, T., and M. Bode. 2017. "Roman silver objects from the ancient kingdom of Kartli (Caucasian Iberia) in Georgia (Mtskheta, Dedoplis Gora [Kareli district]) – a Lead Isotope Investigation." *Metalla* 23, no. 2: 39–50.

Pomiès, C., A. Cocherie, C. Guerrot, E. Marcoux, and J. Lancelot. 1988. "Assessment of the precision and accuracy of lead-isotope ratios measured by TIMS for geochemical applications: Example of massive sulphide deposits (Rio Tinto, Spain)." *Chemical Geology* 144, no. 1: 137–149.

Reimer, P., W. Austin, E. Bard, A. Bayliss, P. Blackwell, C. Bronk-Ramsey, M. Butzin, H. Cheng, R. L. Edwards, M. Friedrich, P. M. Grootes, T.P. Guilderson, I. Hajdas, T. Heaton, A. G. Hogg, K. A. Hughen, B. Kromer, S. W. Manning, R. Muscheler, J. G. Palmer, C. Pearson, J. Van der Plicht, R. W. Reimer, D. A. Richards, E. M. Scott, J. R. Southon, C. S. M. Turney, L. Wacker, F. Adolphi, U. Büntgen, M. Capano, S. M. Fahrni, A. Fogtmann-Schulz, R. Friedrich, P. Köhler, S. Kudsk, F. Miyake, J. Olsen, F. Reinig, M. Sakamoto, A. Sookdeo, and S. Talamo. 2020. "The IntCal20 Northern Hemisphere radiocarbon age calibration curve (0–55 cal kBP)." *Radiocarbon* 62, no. 4: 725–57.

Renberg, I., R. Bindler, and M.-L. Brännvall. 2001. "Using the historical atmospheric lead- deposition record as a chronological marker in sediment deposits in Europe." *The Holocene* 11, no. 5: 511–16.

Rohl, B. 1996. "Lead isotopes data from the isotrace laboratory, Oxford: Archaeometry data 2, galena from Britain and Ireland." *Archaeometry* 38: 165–80.

Rosman, K. J. R., W. Chisholm, S. Hong, J. P. Candelone, and C. F. Boutron. 1997. "Lead from Carthaginian and Roman Spanish mines isotopically identified in Greenland ice dated from 600 BC to 300 AD." *Environmental Science and Technology* 31, no. 12: 3413–16.

Rothenhöfer, P., N. Hanel, and M. Bode. 2017. "Bleicistae mit Produzenteninschriften aus dem römischen Schiffswrack von Rena Maiore (Sardinien). Arelate/Arles (Dép. Bouches-du-Rhône/F) als Umschlagplatz im überregionalen Metallhandel?" *Archäologisches Korrespondenzblatt* 47, no. 2: 217–29.

Ruiz, C., A. Arribas, and A. ArribasJr. 2002. "Mineralogy and geochemistry of the Masa Valverde blind massive sulphide deposit, Iberian Pyrite Belt (Spain)." *Ore Geology Review* 19, no. 1: 1–22.

Salel, T., H. Bruneton, J.-P. Degeai, L. Dolez, M. Mulot, and D. Lefèvre. 2019. "Enregistrement sédimentaire de paléo-pollutions au plomb dans la basse vallée de l'Aude." In *Paysages pour l'homme, Actes du colloque international en hommage à Paul Ambert*, ed. M. Laroche, L. Bruxelles, P. Galant, and M. Ambert, 133–39. Cabrières: Association Culturelle des Amis de Cabrières.

Sangster, D. F., P. M. Outridge, and W. J. Davis. 2000. "Stable lead isotope characteristics of lead ore deposits of environmental significance." *Environmental Reviews* 8, no. 2: 115–47.

Scrinzi, M., C. Flaux, H. Djerbi, C. Vaschalde, M. Tillier, A. Renaud, S. Save, A. Malignas, E. Doyen, N. Caballero, and M. Errera. 2021. *Aménagement, franchissement et morphogénèse d'un cours d'eau dans la proche campagne nîmoise de l'âge du Fer à nos jours. Le Vistre de la Fontaine 2-2 (Nîmes, 30)*. Cournonterral: Mosaïques Archéologie.

Shotyk, W., M. Krachler, A. Martinez-Cortizas, A. K. Cheburkin, and H. Emons. 2002. "A peat bog record of natural, pre-anthropogenic enrichments of trace elements in atmospheric aerosols since 12,370.sup.14C yr BP, and their variation with Holocene climate change." *Earth and Planetary Science Letters* 199, no. 1: 21–37.

Stanley, J.-D., R. W. Carlson, G. Van Beek, T. F. Jorstad, and E. A. Landau. 2007. "Alexandria, Egypt, before Alexander the Great: A multidisciplinary approach yields rich discoveries." *GSA Today* 17, no. 8: 4–10.

Stock F., M. Knipping, A. Pint, S. Ladstätter, H. Delile, A. G. Heiss, H. Laermanns, P. D. Mitchell, R. Ployer, M. Steskal, U. Thanheiser, R. Urz, V. Wennrich, and H. Brückner. 2016. "Human impact on Holocene sediment dynamics in the eastern Mediterranean – the example of the Roman harbour of Ephesus." *Earth Surface Processes and Landforms* 41, no. 7: 980–96.

Stos-Gale, Z. A., and N. H. Gale. 2009. "Metal provenancing using isotopes and the Oxford archaeological lead isotope data base (OXALID)." *Archaeological and Anthropological Sciences* 1, no. 3: 195–213.

Stos-Gale, Z. A., N. H. Gale, and N. Annetts. 1996. "Lead isotope data from the Isotrace Laboratory, Oxford: Archaeometry data base 3, ores from Aegean, part 1." *Archaeometry* 38, no. 2: 381– 90.

Stos-Gale, Z.A., N. H. Gale, J. Houghton, and R. Speakman. 1995. "Lead isotope data from the Isotrace Laboratory, Oxford: Archaeometry data base 1, ores from western Mediterranean." *Archaeometry* 37, no. 2: 407–15.

Swainbank, I. G., T. J. Shepherd, R. Caboi, R. Masssoli-Novelli. 1982. "Lead isotopic composition of some galena ores from Sardinia." *Periodico di Mineralogia* 51, no. 3: 275–86.

Tillier, M. 2019. *Économie végétale et échanges en Méditerranée romaine (1er s. av. n.-è. – 5ème s. de n.è.). Étude carpologique de contextes portuaires*. PhD diss., Univ. Paul Valéry Montpellier 3.

Véron, A., J.-P. Goiran, C. Morhange, N. Marriner, and J.-Y. Empereur. 2006. "Pollutant lead reveals the pre-Hellenistic occupation and ancient growth of Alexandria, Egypt." *Geophysical Research Letters* 33, no. 6: 1–4.

Véron, A., C. Morhange, A. Poirier, B. Angeletti, and F. Bertoncello. 2018. "Geochemical markers of human occupation in the lower Argens valley (Fréjus, France): From protohistory to Roman times." *JAS: Reports* 17: 242-49.

Veyrac, A. 2006. *Nîmes romaine et l'eau*. Paris: CNRS éditions.

Wagner, G. A., W. Gentner, O. Muller, N. H. Gale. 1979. *Chemical and Lead Isotope Analyses of Ores from the Ancient Silver Mines on Siphnos*. London: 19th International Symposium on Archaeometry.

WHO/FAO. 2001. *Codex Alimentarius Commission. Food Additives and Contaminants*. Food Standards Program, ALINORM 10/12A.